

Integrated Transformers With Magnetic Thin Films

Hao Wu¹, Michael Lekas¹, Ryan Davies¹, Kenneth L. Shepard^{1,2}, *Fellow, IEEE*, and Noah Sturcken¹

¹Ferric Inc., New York, NY 10027 USA

²Department of Electrical Engineering, Columbia University, New York, NY 10027 USA

This paper presents the design and electrical performance of transformers with magnetic thin films for on-chip power conversion and isolation. The inductance of the devices is greatly enhanced by the use of a high-permeability magnetic material as a solenoid core, resulting in an inductance density of 108 nH/mm^2 . The total thickness of the transformer structures is $<30 \mu\text{m}$ with a volume inductance density of $3.6 \mu\text{H/mm}^3$. By laminating the magnetic core, losses are well controlled leading to a peak quality factor (Q) of 16 at 40 MHz.

Index Terms—Integrated magnetic devices, magnetic thin films, on-chip transformers, power conversion.

I. INTRODUCTION

THE INTEGRATION of high-permeability magnetic thin films with standard CMOS manufacturing assists in the realization of a new class of integrated magnetic components such as inductors, transformers, and transmission lines [1]–[5]. Chip-scale transformers have traditionally been limited to applications that only require small inductance values ($<10 \text{ nH}$), such as RF matching networks and baluns, due to the low inductance densities that can be achieved with on-chip air-core devices. However, the addition of high-permeability magnetic films to a CMOS process allows for the design of transformers with much higher inductance densities than previously achievable with air-core structures. These magnetically enhanced devices enable the monolithic integration of new semiconductor products such as galvanically isolated dc-dc power converters that operate at switching frequencies higher than 10 MHz, and have 100% of their necessary components integrated on-chip [6], [7].

In this paper, we present transformers that exhibit high inductance, coupling coefficient, and current density, and low dc resistance relative to existing integrated microtransformer technologies [8]–[11]. Three transformers were designed with identical footprints, but differing turns ratios to demonstrate the varying impedance ratios that may be designed in the process. Both the magnetic core and final fabricated transformers were characterized independently to aid modeling of the devices. By adopting a high-permeability cobalt alloy thin-film core, high inductance density was achieved reducing the footprint and profile of the integrated transformers. Laminations in the magnetic thin-film core provide a good high-frequency response beyond 100 MHz. In addition to fully integrated, isolated power converters, these transformers will also enable a new set of IC applications such as signal isolation and impedance matching.

II. INTEGRATED TRANSFORMERS DESIGN AND FABRICATION

A. Transformer Design

A solenoid structure was chosen for these integrated transformers to minimize capacitive and inductive coupling

Manuscript received November 6, 2015; revised December 29, 2015; accepted January 3, 2016. Date of publication January 6, 2016; date of current version June 22, 2016. Corresponding author: H. Wu (e-mail: hao.wu@ferricsemi.com).

Color versions of one or more of the figures in this paper are available online at <http://ieeexplore.ieee.org>.

Digital Object Identifier 10.1109/TMAG.2016.2515501

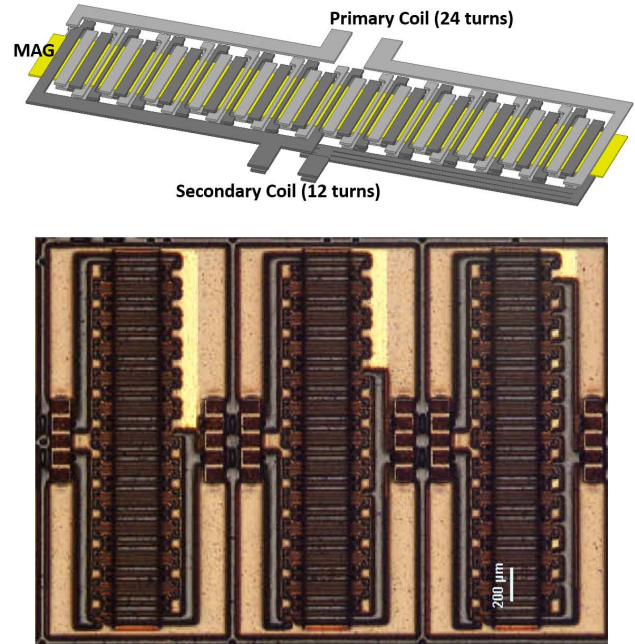


Fig. 1. Top: 3-D design of 2:1 transformer where MAG is the magnetic core around which the transformer coils are wound. Bottom: microscope image of integrated transformers as fabricated on Si substrate. Each turn of the primary coil is identical, whereas the secondary coil windings vary to achieve different turns ratio. From left to right, transformer design (i), (ii), and (iii). The scale bar is $200 \mu\text{m}$.

between devices and the silicon substrate. Unlike a spiral-type structure, the magnetic flux generated by a solenoid is parallel to the substrate and most of the flux is confined to the high-permeable magnetic core. To fully utilize the magnetically anisotropic magnetic core and increase its overall permeability, the transformers were elongated in the hard-axis direction [the vertical direction in the microscope image shown in Fig. 1 (bottom)]. A 3-D illustration of a 2:1 transformer design is shown in Fig. 1 (top). The primary coil consists of 24 turns and the secondary coil has two sets of 12 turns in parallel, both of which are fully interleaved with the primary coil. By changing the wiring connection in the secondary coil, different turns ratio can be easily implemented, as shown in Fig. 1 (bottom). Detailed transformer design parameters are listed in Table I.

B. Transformer Fabrication

Integrated transformers were fabricated at Taiwan Semiconductor Manufacturing Company on 300 mm wafers in

TABLE I
TRANSFORMER DESIGN PARAMETERS

	Design (i)	Design (ii)	Design (iii)
Turns ratio	2:1	3:1	12:1
Primary Turns	24	24	24
Secondary Turns	12	8	2
Winding Width, μm	40	40	40
Winding Thickness, μm	9	9	9
Winding Spacing, μm	15	15	15
Core dimension, μm	300×2200	300×2200	300×2200
Device dimension, μm	712×2286	712×2286	712×2286

a pilot manufacturing line using standard CMOS manufacturing equipment and processes. The details of fabrication process can be found in [1]. The transformer consists of three metal layers separated by insulators that include a bottom copper layer, a top copper layer, and the magnetic core layer (MAG, as shown in Fig. 1) in between. For characterization, inductors were fabricated on test vehicle wafers that had not undergone CMOS front-end processes. Passivation and wafer finishing steps necessary for commercial CMOS wafers were completed on the test vehicle wafers and, consequently, the performance demonstrated on the test vehicle will be consistent with the inductors fabricated on commercial CMOS wafers.

III. EXPERIMENTS AND RESULTS

A. Magnetic Core

The magnetic core is a composite of amorphous cobalt alloy and insulating laminations to suppress eddy currents and improve frequency response. A vibrating sample magnetometer and B - H loop tracer were used for characterizations. The bulk magnetic core material has a coercivity < 1 Oe and saturation magnetization $\sim 15\,000$ G. B - H loop measurements [1] indicate that a uniaxial anisotropy was induced in the magnetic core and the anisotropy field is ~ 20 Oe. The hard-axis relative permeability is then calculated as B_s/H_k to be ~ 750 . In order to investigate the high-frequency response of the permeability, frequency-dependent permeability was measured on a $50\ \Omega$ stripline testing structure [12]. The initial measurement was performed on a coupon of unpatterned magnetic film that was $10\ \text{mm} \times 10\ \text{mm} \times 0.005\ \text{mm}$. Fig. 2 shows the permeability measurement results. The real component of the permeability of the unpatterned film starts rolling off at approximately 20 MHz due to the induced eddy currents in the magnetic film. The frequency-dependent permeability μ_r may be analytically calculated as [13]

$$\mu_r = \mu_i \frac{(1-i)}{d/\delta} \frac{e^{(1+i)d/\delta} - 1}{e^{(1+i)d/\delta} + 1} \quad (1)$$

where μ_i is the intrinsic permeability, d is the film thickness, and δ is the skin depth determined by frequency, film resistivity, and permeability. The calculations match well with the measurement results, as shown in Fig. 2.

Since the film will be patterned into long rectangular shapes in actual applications, a patterned sample of the same dimensions was also measured, which shows a large real permeability up to ~ 1.4 GHz (Fig. 2). The decrease in real permeability of the patterned film relative to the unpatterned

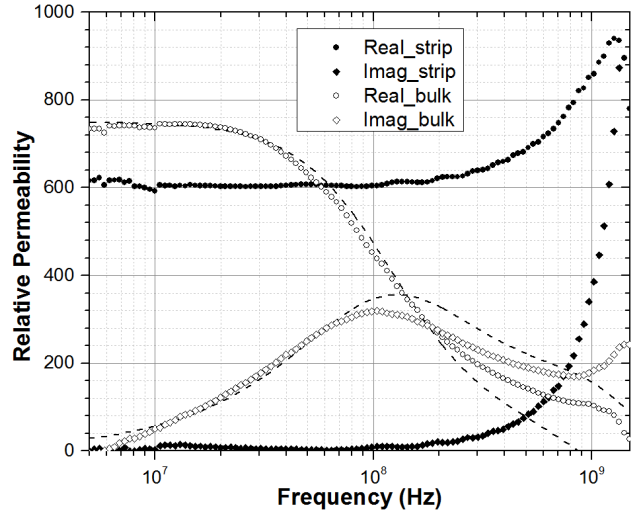


Fig. 2. Measured permeability on $5\ \mu\text{m}$ -thick unpatterned magnetic thin film (open dots) and patterned magnetic film (solid dots). Dashed lines: theoretical values calculated from analytical equation (1).

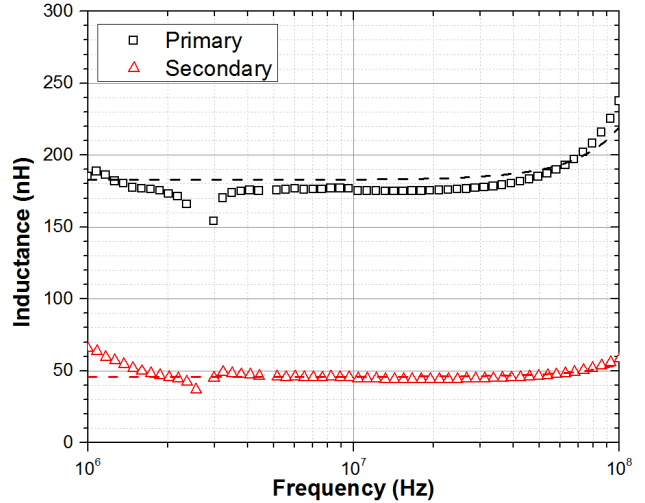


Fig. 3. Measured inductance (L) of transformer design (i). Dashed lines: simulation results from ANSYS HFSS 3-D EM simulator that are consistent with measured data.

film is due to demagnetizing effects. The effective permeability is then given by [14]

$$\mu_{\text{eff}} = \frac{\mu_r}{1 + N_d(\mu_r - 1)} \quad (2)$$

where N_d is the demagnetizing factor [15].

Combining (1) and (2), the frequency-dependent permeability can be calculated for magnetic cores with arbitrary shapes. The calculated value was then used in ANSYS HFSS 3-D EM simulator Electromagnetic (EM) to simulate designed transformers, and the results were found to be consistent with the experimental data (Fig. 3).

B. Transformers With Different Turns Ratio

DC resistance was obtained by four-point Kelvin measurements to avoid the addition of the parasitic resistance in the device leads and contact resistance. Four-port s-parameters

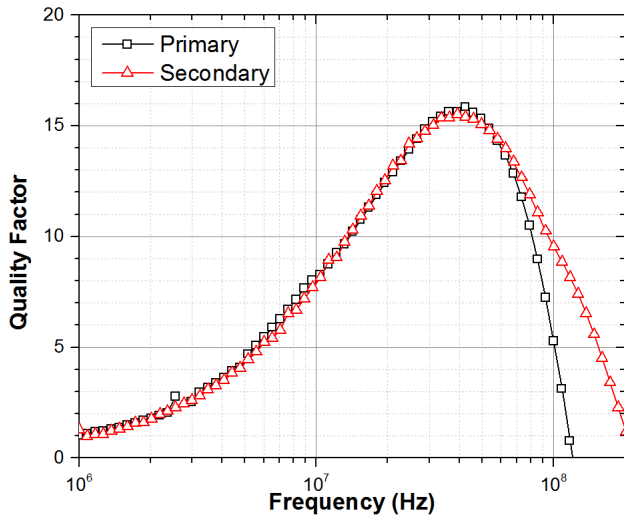


Fig. 4. Measured quality factor (Q) of transformer design (i). The peak Q is as high as 16 at 40 MHz.

were measured using an Agilent N5230A vector network analyzer and a Cascade probe station with G-S-G-S-G probes.

As shown in Fig. 3, the measured inductance of the primary and secondary coils are 175 and 44 nH, respectively. For an ideal transformer with perfect coupling, the turns ratio is equal to the square root of the ratio of the primary and secondary inductances. Accordingly, the turns ratio of transformer design (i) was calculated as 1.994, which is very close to 2 indicating a very low leakage inductance. HFSS simulations showed that an identical design with an air core has a primary inductance of 5.8 nH and a secondary inductance of 1.4 nH. Therefore, the inductance was enhanced by more than 30 \times due to the magnetic thin-film core. Moreover, the self-resonant frequency for both the primary and secondary coils is greater than 100 MHz, which provides a suitable frequency band for high-frequency switch-mode power conversion applications. The quality factor has a maximum value of 16 around 40 MHz, as shown in Fig. 4.

The saturation current of each coil of the transformer was obtained by applying a dc current to one coil using an RF bias tee and measuring the s-parameters, while leaving the opposite coil open circuited. Fig. 5 shows the inductance as a function of the applied dc current for both the primary and secondary coils of design (i). The inductance starts to decrease as the dc current exceeds 200 mA. The saturation current of design (i) is 300 mA, which is defined as the dc current at which the inductance decreases by 20%. Fig. 6 shows coupling coefficient (k) and maximum available gain (G_{\max}), which are also the useful figure of merit of integrated transformers [16]. By definition, G_{\max} indicates the power transfer efficiency of integrated transformers.

Table II lists design parameters and electrical performance for the three transformer designs. As turns ratio increases, the coupling coefficient decreases due to the increasing leakage inductance. For the same reason, the inductance of the primary coils decreases leading to a decrease in peak quality factor. This indicates that high turns ratio is achieved with some compromise in electrical performance. A high turns ratio may be realized with a single device, or a series of cascaded

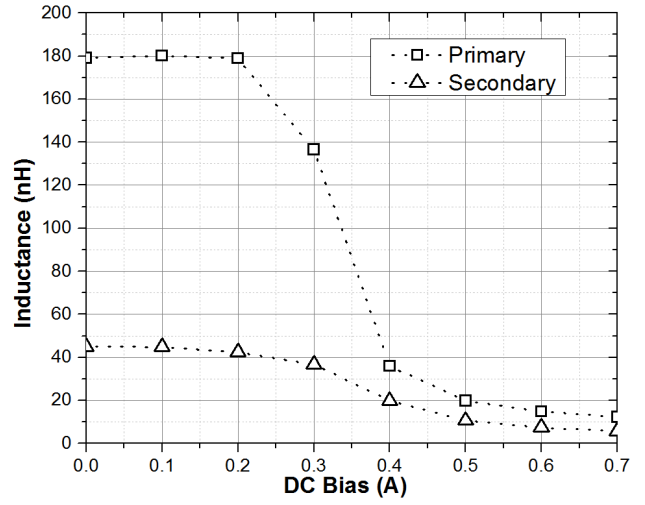


Fig. 5. Inductance versus applied dc bias of transformer design (i). The saturation current is defined as current when L drops by 20%, which is ~ 300 mA in this plot.

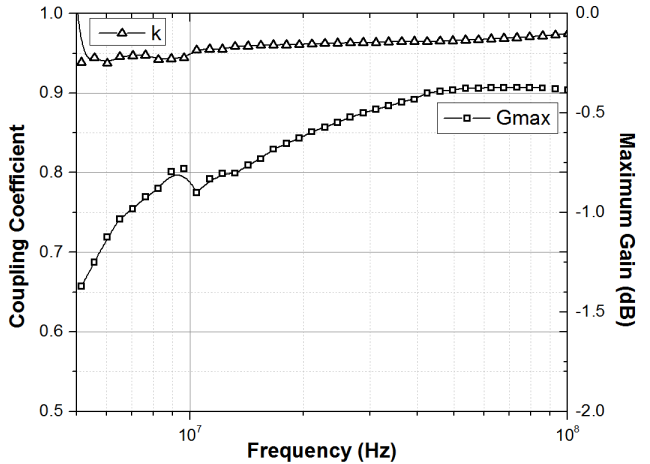


Fig. 6. Coupling coefficient and maximum available gain of transformer design (i).

TABLE II
ELECTRICAL PERFORMANCE OF TRANSFORMER DESIGNS

	Design (i)	Design (ii)	Design (iii)
Turns ratio	2:1	3:1	12:1
DC resistance, Ω	1.35, 0.34 ^a	1.36, 0.17	1.39, 0.02
Inductance, nH	175, 44 ^a	166, 19	151, 2
Peak Q	16	14	11
Frequency, MHz	up to 80	up to 80	up to 100
Coupling coefficient	0.96	0.95	0.74
Saturation current, mA	300	300	300

Inductance and coupling coefficient were extracted at 20 MHz. The saturation current is defined as the current level when inductance drops by 20%.

^a Primary, Secondary

transformers with lower turns ratio depending on the specific requirements of the application.

In Table III, the electrical performance of published integrated transformers is listed for comparison. High-inductance values were basically achieved by large volume

TABLE III
COMPARISON OF INTEGRATED TRANSFORMER PERFORMANCE

Transformer Type	DC resistance Ω	Inductance nH	Frequency MHz	Peak Q	Coupling	Gain dB	L/area nH/mm ²	L/volume $\mu\text{H}/\text{mm}^3$
[3]	Solenoid	5.4	565	40	6.3	0.97	--	--
[8]	Solenoid	0.35	12-116	40	3	--	--	23
[9]	Solenoid	--	1.5-2.5	3000	14	0.65	-9	15
[10]	Solenoid	1.2	53	50	3	0.9	-7	11
[17]	Solenoid	--	40,000	1	7.1	0.97	--	--
[18]	Spiral	0.45	88	20	5.9	0.98	--	44
[19]	Spiral	1.22	270	30	--	0.9	-1	90
This work	Solenoid	1.35	175	100	16	0.96	-0.6	108
								3.6

The inductance, coupling coefficient and Gain were extracted at 20 MHz for this work.

of magnetic materials which in turn limits the frequency response [3], [17], [19]. Gao *et al.* [9] reported an ultra-high-frequency range; however, the inductance enhancement was compromised. The transformers in this paper are superior in inductance density, peak quality factor, and frequency. This demonstrates that these transformers can be used in a wide variety of applications.

IV. CONCLUSION

In this paper, integrated transformers with thin-film magnetic cores fabricated with the standard CMOS manufacturing technology were presented. These devices have the highest known volume inductance density of any published result for a monolithic transformer, and are available in commercial CMOS, making them a viable technology option for the design of fully integrated switched-mode dc-dc converters. In addition, transformers with lower capacitive parasitics and varying inductance can be designed in this process technology through careful layout and simulation to accommodate higher frequencies of operation for applications like RF impedance matching and single-ended to differential signal conversion.

ACKNOWLEDGMENT

This work was supported by the Department of Energy under Award DE-SC0009200. The author would like to thank K. W. Cheng, C. C. Chen, Y. S. Su, C. Y. Tsai, K. D. Wu, J. Y. Wu, Y. C. Wang, K. C. Liu, C. C. Hsu, C. L. Chang, W. C. Hua, and A. Kalnitsky from Taiwan Semiconductor Manufacturing Company for device fabrication and process support. They would also like to thank A. Roth, E. Soenen, and Prof. L. Pileggi for the insight and support.

REFERENCES

- N. Sturcken *et al.*, "Magnetic thin-film inductors for monolithic integration with CMOS," in *Proc. IEEE Int. Electron Devices Meeting*, Dec. 2015, pp. 11.4.1–11.4.4.
- D. S. Gardner, G. Schrom, F. Paillet, B. Jamieson, T. Karnik, and S. Borkar, "Review of on-chip inductor structures with magnetic films," *IEEE Trans. Magn.*, vol. 45, no. 10, pp. 4760–4766, Oct. 2009.
- J. Mullenix, A. El-Ghazaly, and S. X. Wang, "Integrated transformers with sputtered laminated magnetic core," *IEEE Trans. Magn.*, vol. 49, no. 7, pp. 4021–4027, Jul. 2013.
- H. Wu, S. Zhao, D. S. Gardner, and H. Yu, "Improved high frequency response and quality factor of on-chip ferromagnetic thin film inductors by laminating and patterning Co-Zr-Ta-B films," *IEEE Trans. Magn.*, vol. 49, no. 7, pp. 4176–4179, Jul. 2013.
- N. Wang *et al.*, "Integrated on-chip inductors with electroplated magnetic yokes (invited)," *J. Appl. Phys.*, vol. 111, no. 7, p. 07E732, 2012.
- C. R. Sullivan, D. V. Harburg, J. Qiu, C. G. Levey, and D. Yao, "Integrating magnetics for on-chip power: A perspective," *IEEE Trans. Power Electron.*, vol. 28, no. 9, pp. 4342–4353, Sep. 2013.
- C. Ó. Mathúna, N. Wang, S. Kulkarni, and S. Roy, "Review of integrated magnetics for power supply on chip (PwrSoC)," *IEEE Trans. Power Electron.*, vol. 27, no. 11, pp. 4799–4816, Nov. 2012.
- D. Dinulovic, M. Kaiser, A. Gerfer, O. Opitz, M. C. Wurz, and L. Rissling, "Microtransformer with closed Fe-Co magnetic core for high frequency power applications," *J. Appl. Phys.*, vol. 115, no. 17, p. 17A317, 2014.
- Y. Gao *et al.*, "High quality factor integrated gigahertz magnetic transformers with FeGaB/Al₂O₃ multilayer films for radio frequency integrated circuits applications," *J. Appl. Phys.*, vol. 115, no. 17, p. 17E714, 2014.
- X. Xing, N. X. Sun, and B. Chen, "High-bandwidth low-insertion loss solenoid transformers using FeCoB multilayers," *IEEE Trans. Power Electron.*, vol. 28, no. 9, pp. 4395–4401, Sep. 2013.
- B. Chen, "Fully integrated isolated DC-DC converter using micro-transformers," in *Proc. 23rd Annu. IEEE Appl. Power Electron. Conf. Expo.*, Feb. 2008, pp. 335–338.
- D. Pain, M. Ledieu, O. Acher, A. L. Adenot, and F. Duverger, "An improved permeameter for thin film measurements up to 6 GHz," *J. Appl. Phys.*, vol. 85, no. 8, pp. 5151–5153, 1999.
- E. van de Riet and F. Roozeboom, "Ferromagnetic resonance and eddy currents in high-permeable thin films," *J. Appl. Phys.*, vol. 81, no. 1, pp. 350–354, 1997.
- D. W. Lee, K.-P. Hwang, and S. X. Wang, "Fabrication and analysis of high-performance integrated solenoid inductor with magnetic core," *IEEE Trans. Magn.*, vol. 44, no. 11, pp. 4089–4095, Nov. 2008.
- A. Aharoni, L. Pust, and M. Kief, "Comparing theoretical demagnetizing factors with the observed saturation process in rectangular shields," *J. Appl. Phys.*, vol. 87, no. 9, pp. 6564–6566, 2000.
- K. T. Ng, B. Rejaei, and J. N. Burghartz, "Substrate effects in monolithic RF transformers on silicon," *IEEE Trans. Microw. Theory Techn.*, vol. 50, no. 1, pp. 377–383, Jan. 2002.
- A. Moazenzadeh, F. S. Sandoval, N. Spengler, V. Badilita, and U. Wallrabe, "3-D microtransformers for DC-DC on-chip power conversion," *IEEE Trans. Power Electron.*, vol. 30, no. 9, pp. 5088–5102, Sep. 2015.
- R. Wu, N. Liao, X. Fang, and J. K. O. Sin, "A silicon-embedded transformer for high-efficiency, high-isolation, and low-frequency on-chip power transfer," *IEEE Trans. Electron Devices*, vol. 62, no. 1, pp. 220–223, Jan. 2015.
- N. Wang, R. Miftakhutdinov, S. Kulkarni, and C. O'Mathuna, "High efficiency on Si-integrated microtransformers for isolated power conversion applications," *IEEE Trans. Power Electron.*, vol. 30, no. 10, pp. 5746–5754, Oct. 2015.